An Oceanic Front : The Formation of Tidal Fronts with Its Microscale Structure Evolution

Yi-Gn Noh

Department of Astronomy and Atmospheric Sciences, Yonsei University, Seoul, Korea

(Manuscript received 22 October 1993)

해양전선 : 조석전선의 형성 및 그 미세구조의 전개 과정

노의근

연세대학교 천문대기과학과

(1993년 10월 22일 접수)

요 약

해양에서의 전선형성에 관해 그 발생기작을 중심으로 검토되었으며, 특히 조석혼합에 의해 발생하는 연안전선의 발생기작이 조석전선 형성에 관계되는 미세구조의 변화를 포함하는 연안의 해수 수직면에 대한 일차원 모형을 통해 이해되었다. 이로부터 조석전선의 형성을 예측하는 새로운 기준을 설정하였다. 모형으로부터 계산된 해수의 밀도 및 난류에너지의 시간에 따른 발달은 수온약층의 형성하기 위한 조건은 δ가 클 때는 ($\delta > 0.5$) $R\delta^{-}$ constant로서 주어지지만, δ가 0에 접근함에 따라 δ에 점점 무관하게 됨을 보여준다. 여기서, $R=H^4Q/K_b^3$, $\delta=1-D_0/H$, Q는 해수면에서의 부력속, K_b는 해저에서의 와확산 계수, D_0는 해저에서 조석혼합이 없을 경우의 수온약층의 깊이이다. 주어진 D_0 아래서 수온약층의 깊이는 조석혼합이 증가함에 따라 감소하는 것이 발견되었다. 그 결과는 기존의 연구와 비교 검토되었다.

Abstract

The basic processes responsible for the generation of oceanic fronts were reviewed. In particular the process of a shelf sea front produced by tidal stirring was identified from the one dimensional model of the water column in the coastal area, which incorporates the microscale process for the formation of a tidal front. Also a new criterion to predict its location was suggested. The time evolutions of the distributions of density and turbulent kinetic energy calculated from the model show that the criterion for the formation of a thermocline can be predicted as $R\delta^4 \sim$ constant for large δ ($\delta > 0.5$), but the dependence on δ decreases as δ goes to O, where $R=H^4Q/K_b^3$, $\delta=1-Do/H$, Q is the buoyancy flux at the surface, K_b is the eddy diffusivity maintained at the bottom and Do is the depth of a thermocline in the absence of bottom mixing. The depth of a thermocline was found to decrease as the bottom mixing increases for a given value of Do. The results were interpreted in comparison with the previous studies.

1. Review

Fronts are regions of intensified horizontal temperature gradients which occur widely in shelf seas and estuaries. They constitute important features of the structure and circulation and may play a critical role in relation to biological production as well as being of practical importance in problems of waste disposal in coastal seas.

Frontal zones are usually distinguished from the rest of the ocean by the relatively large velocities and velocity gradients which exist there. A feature of most frontal systems is a marked convergence in the horizontal flow usually at the surface. Associated with this convergence is a pattern of pronounced vertical motions making the front an area of enhanced vertical transfer of momentum and other properties. Horizontal velocities, too, tend to be increased, particularly in large-scale fronts where the geostrophic constraints require an along front flow concentrated in the region of horizontal density change.

Fronts may also have practical significance in many practical aspects of the management of the coastal seas. Their presence will modify the circulation and mixing process in ways that may have significant influence on the discharged into coastal waters. The proximity of a frontal zone may therefore be an important consideration in, for example, the siting of a nuclear power station or on offshore dumping operation. For buoyant pollutants the convergence associated with the front certainly inhibit dispersion and lead to a concentration of pollutants along the line of the front.

Fronts occur on all scales, from fractions of a meter to global extent. The largest fronts, formed in regions of convergence of planetary scale winds, have important effects on weather and climate.

Fronts are found in the surface layers, at mid depths, and near the ocean bottom (benthic fronts). Fronts can be conveniently classified into six categories :

1) Fronts of planetary scale, usually associated with the convergence of surface Ekman transports, and found away from major ocean boundaries (e. g., within the Sargasso Sea, Southern Ocean).

2) Fronts representing the edge of major western boundary currents. These fronts are associated with the intrusion of warm, salty water of tropical origin into higher latitudes (e. g., Gulf Stream, Kuroshio).

3) Shelf break fronts formed at the boundary of shelf and slope waters, such as are found in the Middle Atlantic Bight. Circulation along the front may or may not be baroclinic depending on whether the temperature and salinity fronts coincide, and whether their contributions to the density field are compensating or reinforcing.

4) Upwelling fronts, essentially the surface manifestation of an inclined pycnocline, commonly formed during a coastal upwelling, i. e. as a result of an offshore surface Ekman transport associated with alongshore wind stresses (e. g., along the west coast of the U. S., Peru, Northwest and Southwest Africa).

5) Plume fronts at the boundaries of riverine plumes discharging into coastal waters (e. g., Amazon, Columbia, Hudson, Conneticut, etc.).

6) Tidal fronts, formed in continental seas and estuaries, and around islands, banks, capes and shoals. These are commonly located in the boundary regions between shallow wind and tidally mixed nearshore waters and stratified, deeper, offshore waters (e. g., Celtic and Irish Seas, approaches to English Channel, Long Island Sound).

All of these frontal systems share common properties of persistence, ranging from hours to months in spite of diffusion of properties across strong horizontal gradients, and surface convergence with associated strong vertical convection, usually at least an order of magnitude greater than open ocean vertical convection.

The component of flow parallel to fronts frequently has intense horizontal shear in a

direction normal to the fronts. Such shears may be in a geostrophic equilibrium for the larger fronts, but flows near shallow water, small scale fronts are expected to be more strongly influenced by local acceleration, bottom stress, and by interfacial friction that Coriolis force.

In this paper, attention is restricted to the last case.

2. Tidal fronts

In coastal regions of the ocean where the relatively shallow shelf occupies large areas, the turbulence generated from the tidal friction causes the formation of a sharp structure between the well-mixed shelf water and the two-layer stratified water in the deeper regions adjacent to the shelf (Figure 1). To predict the position of such fronts, Simpson and Hunter (1974) proposed the criterion using the parameter R*, which determines whether the water column is well-mixed or stratified. The parameter R* was obtained by the balance between the rate of turbulent kinetic energy supply to maintain vertical homogeneity of the water column against the continuous stratifying effect of the buoyancy flux to the energy dissipation rate of tidal flows due to near bottom friction, which gives.

$$R^* = QH / U_t^3 \qquad (2.1)$$

where Q is the buoyancy flux at the surface, H is the depth of the sea and U_t is the amplitude of tidel velocity. When R* is small in the the shallow water ($R^* < 10^5$, Simpson et al. 1978), the sea water maintains a well-mixed state with relatively uniform vertical density distribution, and the heat supplied on the surface is effectively transferred to the bottom. On the other hand, when R* becomes larger with the increase of the water depth, there appears a thermocline and this makes the temperature at the sea surface much higher compared to the well-mixed state by prohibiting the vertical heat transfer. The boundary between the cool well-mixed water and the warm stratfied water leads to the formation of a tidal front at the sea surface as shown in Figure 1.

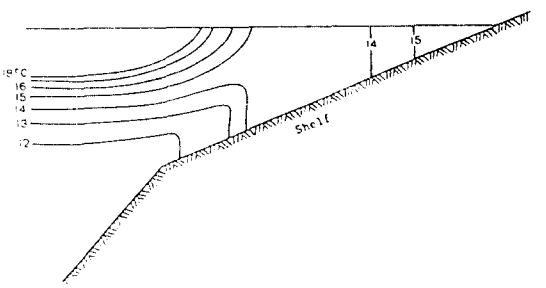

Fig. 1. A schematic view of the transverse structure of the tidal front (from Fedorov (1983)).

There have been numerous studies on the tidal front formation (Fearnhead 1975, Simpson et al. 1978, Pingree and Griffiths 1978, Bye 1990). All the previous models, however, are based on the global balance between the input of kinetic energy from the tidal friction and the demand of potential energy required to prevent stratification in the water column. The study by turbulence modeling, in which the internal structure of the water column can be acquired, has not been carried out. In particular, the interaction between turbulence structure and buoyancy flux, which leads to the stratification or the destratification of the mixed layer, is not clearly understood yet.

If the stabilizing buoyancy is imposed on the surface of a turbulent fluid, the turbulence is suppressed by the stratification of the fluid, and the eddy diffusivity is reduced. The local reduction of the eddy diffusivity is capable of inducing even stronger stratification at a certain depth, where the turbulence is suppressed further. This mechanism always leads to the formation of a thermocline across which both the propagations of turbulent kinetic energy and the buoyancy flux are prohibited, when turbulence is generated only at the surface (Noh and Fernando 1991a). If turbulence is generated both at the surface and at the bottom, however, the kinetic energy supply from the bottom helps to keep the eddy diffusivity at a certain level at the position of potential thermocline formation.

The turbulent kinetic energy flux from the bottom, if it becomes sufficiently strong, may prohibit the feedback mechanism leading to the formation of a thermocline, thus maintaining a well-mixed state without forming a thermocline.

The Simpson and Hunter's criterion given by (2. 1) applies only to the situation where the bottom mixing-the turbulence generation by the tidal friction at the bottom is predominatnt in comparison with the surface mixing the turbulence generation by wind shear at the sea surface, so that the surface mixed layer is very thin compared to the water depth. Nevertheless the importance of surface mixing is evident from the critical role in the formation of a thermocline as mentioned above, although its effects is often obscured by the fact that the wind field does not vary significantly over the large area in the sea (Simpson et al. 1978). The contributions of the wind stress have been often included in previous models (for example, Simpson et al. 1978, Fearnhead 1975), but its effects on the formation of a thermocline is not properly explained yet.

The mechanism for the tidal front formation has been also investigated using the laboratory experiments by Hopfinger and Linden (1982). In their experiments the stabilizing buoyancy flux (by heat) is imposed on the water surface and the shear-free turbulence is generated by the oscillation of a grid located near the bottom. They observed that the surface temperature increases much faster than that expected from the uniform mixing over the whole water column, if the stratification criterion

$$R = QH^4 / K_b^3 > A_1 \qquad (2.2)$$

is satisfied, where K_b is the eddy diffusivity at the bottom and A_1 is a constant. The parameter R was modified as

$$R_u = QH / u_u^3 > A_2 \qquad (2.3)$$

using the fact that the local r. m. s. turbulent velocity u is given by $u \sim K_0/z$ for the turbulence generated by the grid-oscillation, where z is the vertical distance from the gridoscillation at the bottom and $u_u = u(z=H)$ and A_2 is a constant. Assuming that u_u is proportional to U_t, Hopfinger and Linden (1982) suggested that (2. 3) is equivalent to (2. 1) with $u_u = 2\times10^{-2}$, which is obtained based on the experimental result such as $A_2 = 1.5$. The realistic two-layer system with a thermocline at a certain depth, as shown in Figure 1, could not not be produced during their experiments, however. Instead the temperature within the thin surface layer ran away, because turbulence was not generated at the surface. This further corroborates the importance of surface mixing.

Therefore, in the present research one-domensional turbulence model, in which the interaction between turbulence and stratification of the fluid is taken into account, is developed to understand the formation of a thermocline within the water column and the consequent formation of a tidal front.

3. Formulation of Mathematical Model

The mean kinetic energy of turbulence (TKE) equation in the absence of a mean shear, can be written as

$$\frac{\partial E}{\partial t} = -\frac{\partial}{\partial z}\left[\overline{w'\left(\frac{p'}{\rho_0}+\frac{u_i'u_i'}{2}\right)}\right] - \overline{w'b'} - \varepsilon, \qquad (3.1)$$

where horizontal homogeneity is assumed. Here $u_i'(i=1,2,3)$ is the fluctuating velocity ($u_3' = w'$), E is the kinetic energy of turbulence ($=\frac{1}{2}\overline{u_i'u_i'}$), b' is the fluctuating buoyancy ($=g\rho'/\rho_0$), ρ' and p' are the fluctuations of density and pressure, ρ_0 is the reference density, g is the gravitational acceleration, and ε is the dissipation rate of TKE. The first and second terms on the RHS of (3. 1) represent the turbulent diffusion of TKE and the buoyancy flux, respectively.

It is well known that the governing equations for the velocity field induced by two independent oscillating boundaries can be represented by the superposition of the ve-

locity fields induced by the individual oscillating boundaries, if the oscillating amplitudes are much smaller than the length scale of the flow, because the nonlinear inertia is negligible compared with the temporal variation of the velocity field (see, for example, Batchelor 1967). In accordance with this it is possible to assume that the turbulent velocity fields induced from these independent velocity fields are also independent each other and the turbulent velocity field can be represented by the superposition of the two turbulent velocity fields generated by the grid-oscillations at the bottom u'_{bi} and the surface u'_{si}. That is,

$$u'_i = u'_{si} + u'_{bi}, \tag{3.2}$$

which are very weakly correlated, i.e.,

$$\overline{u'_{si}u'_{bi}} \ll \overline{u'_{si}u'_{si}} \quad (\text{or } \overline{u'_{bi}u'_{bi}}) \tag{3.3}$$

and

$$\overline{w'_s u'_{bi}u'_{bi}} \quad (\text{or } \overline{w'_b u'_{si}u'_{si}} \ll \overline{w'_b u'_{bi}u'_{bi}} \quad (\text{or } \overline{w'_s u'_{si}u'_{si}}). \tag{3.4}$$

Actually it has been found from the laboratory experiments that the turbulent velocities originated from two different grid oscillations can be considered statistically independent (Turner 1986).

It is then possible to decompose (3.1) into the equation for TKE originated from the surface and that for TKE from the bottom as

$$\frac{\partial E_s}{\partial t} = -\frac{\partial}{\partial z}\overline{\left[w'_s\left(\frac{p'}{\rho_0} + \tfrac{1}{2}u'_{si}u'_{si}\right)\right]} - \overline{w'_s b'} - \varepsilon_s, \tag{3.5}$$

and

$$\frac{\partial E_b}{\partial t} = -\frac{\partial}{\partial z}\overline{\left[w'_b\left(\frac{p'}{\rho_0} + \tfrac{1}{2}u'_{bi}u'_{bi}\right)\right]} - \overline{w'_b b'} - \varepsilon_b. \tag{3.6}$$

where the subscripts s and b denote the physical quantities corresponding to the turbulence originated from the surface ($z=H$) and from the the bottom ($z=O$).

Introducing the eddy diffusivity for the parameterization of turbulent diffusion of TKE and buoyancy, (3.5) and (3.6) become

$$\frac{\partial E_s}{\partial t} = \frac{\partial}{\partial z}\left(K_s\frac{\partial E_s}{\partial z}\right) + K_s\frac{\partial B}{\partial z} - \varepsilon_s, \tag{3.7}$$

$$\frac{\partial E_b}{\partial t} = \frac{\partial}{\partial z}\left(K_b\frac{\partial E_b}{\partial z}\right) + K_b\frac{\partial B}{\partial z} - \varepsilon_b, \tag{3.8}$$

where B is the mean buoyancy. The eddy diffusivities K_s and K_b and the dissipation rates ε_s and ε_b can be modeled as

$$K_s = c_\mu E_s^{1/2} l_s, \tag{3.9}$$

$$K_b = c_\mu E_b^{1/2} l_b, \tag{3.10}$$

$$\varepsilon_s = c_D E_s^{3/2} l_s^{-1}, \tag{3.11}$$

$$\varepsilon_b = c_D E_b^{3/2} l_b^{-1}, \tag{3.12}$$

if it is assumed that the turbulent fields of u'_s and u'_b have their own respective inertial length scales l_s and l_b, where c_μ and c_D are constants.

Similarly, it is possible to describe the variation of the mean buoyancy B using the turbulent diffusion equations as

$$\frac{\partial B}{\partial t} = -\frac{\partial}{\partial z}\overline{w'b'} \tag{3.13}$$

$$= -\frac{\partial}{\partial z}\overline{(w'_s + w'_b)b'} \tag{3.14}$$

$$= \frac{\partial}{\partial z}\left[(K_s + K_b)\frac{\partial B}{\partial z}\right] \tag{3.15}$$

To solve the equations, however, the informations on the velocity and length scales of turbulence are required. Shear-free turbulence generated by oscillating grids, on which the current model is based, has been extensively studied in the laboratory (Hopfinger and Toly 1976, Hannoun et al. 1988) and its numerical simulation has been studied recently by Noh and Fernando (1991a, b). The experimental data show that the integral length scale and the r.m.s. velocity of turbulence in a homogeneous fluid are given by

$$l_b = a_1(z + zo), \tag{3.16}$$

$$u_b = a_2 fS(z + zo)^{-1}, \tag{3.17}$$

When the grid oscillation is located near the bottom, where f and S are the frequency and the stroke of the grid oscillations respectively, and a_1, a_2 and zo are constants that depend on the grid geometry.

Experimental and theoretical studies (Britter et al. 1983, Pearson et al. 1983, Csanady 1964) have shown that, in stably stratified fluids, the growth of the vertical length-scale of turbulence l_{bv} is limited by the buoyancy length-scale l_{bN} ($=u_b/N$, where N is the Brunt -Vaisala frequency). On the basis of these results, it is assumed that l_{bv} has the form

$$l_{bv}=\frac{l_{bn}}{[1+(l_{bn}/(c_l l_{bN}))^2]^{1/2}}, \tag{3.18}$$

where C_e is a constant of order one (Andre et al. 1978, Galperin et al. 1988). If the length scale is rescaled as $l'_{bv}=l_{bv}/a_1$, (3.10) and (3.12) can be written as

$$K_b=c'_\mu E_b^{1/2} l'_{bv}, \tag{3.19}$$

$$\varepsilon_b=c'_D E_b^{3/2} l'^{-1}_{bv}, \tag{3.20}$$

where $c'_\mu=a_1 c_\mu$ and $c'_D=c_D/a_1\varepsilon$.

Similarly the characteristics of the turbulence generated by the grid oscillation near the surface can be described as

$$l_{sn}=a_1(H-z+zo), \tag{3.21}$$

$$u_s=a_2 fS(H-z+zo)^{-1}, \tag{3.22}$$

and the corresponding eddy diffusivity and dissipation rate can be written as

$$K_s=c'\mu E_s^{1/2} l'_{sv}, \tag{3.23}$$

$$\varepsilon_s=c' E_s^{3/2} l'^{-1}_{sv}, \tag{3.24}$$

and the vertical length scale of turbulence under the influence of stratification is given by

$$l_{sv}=\frac{l_{sn}}{[1+(l_{sn}/(c_l l_{sN}))^2]^{1/2}}, \tag{3.25}$$

where $l_{sN}=u_s/N$.

Again the rescaling of t by $t'=c'_\mu t$ μt rewrites (3.7), (3.8) and (3.15) as

$$\frac{\partial E_s}{\partial t'}=\frac{\partial}{\partial z}\left(K'_s\frac{\partial E_s}{\partial z}\right)+K'_s\frac{\partial B}{\partial z}-\left(\frac{c'_D}{c'_\mu}\right)\varepsilon'_s, \tag{3.26}$$

$$\frac{\partial E_b}{\partial t'}=\frac{\partial}{\partial z}\left(K'_b\frac{\partial E_b}{\partial z}\right)+K'_b\frac{\partial B}{\partial z}-\left(\frac{c'_D}{c'_\mu}\right)\varepsilon'_b, \tag{3.27}$$

$$\frac{\partial B}{\partial t'}=\frac{\partial}{\partial z}\left[(K'_S+K'_b)\frac{\partial B}{\partial z}\right], \tag{3.28}$$

where

$$K'_s=E_s^{1/2} l'_{sv}, \tag{3.29}$$

$$\varepsilon'_s=E_s^{3/2} l'^{-1}_{sv}, \tag{3.30}$$

$$K'_b=E_b^{1/2} l'_{bv}, \tag{3.31}$$

$$\varepsilon'_b=E_b^{3/2} l'^{-1}_{bv}. \tag{3.32}$$

For (3.26) and (3.27), $c'_D/c'\mu=6$ can be obtained by subsutituting the characteristic velocity and length scales of turbulence in a homogeneous fluid (3.16) and (3.17) (or (3.21) and (3.22) into the steady-state form of (3.26) (or (3.27)) with $\partial B/\partial z=0$ (Noh and Fernando 1991a). It is important to notice that the equations (3.26)-(2.32) do not include empirical constants any more.

By defining $U=[E_b(0,t')]^{1/2}$ and $L=l'_b(O, t')$, it is possible to define the nondimensional variables as

$$\begin{gathered}E_s^*=\frac{E_s}{U^2},\ l'^*_{sv}=\frac{l'_{sv}}{L},\ E_b^*=\frac{E_b}{U^2},\ l'^*_{bv}=\frac{l'_{bv}}{L},\\ K'^*_s=\frac{K'_s}{(UL)},\ \varepsilon'^*_s=\frac{\varepsilon'_s}{(U^3/L)},\ K'^*_b=\frac{K'_b}{(UL)},\ \varepsilon'^*_b=\frac{\varepsilon'_b}{(U^3/L)},\\ z^*=\frac{z}{L},\ t'^*=\frac{t'}{(L/U)},\ H^*=\frac{H}{L}.\end{gathered} \tag{3.33}$$

The nondimensionalization for B was selected as

$$B^*=\frac{B}{Q/(c'_\mu U)}. \tag{3.34}$$

In what follows, the asterisks denoting the nondimensional variables will be dropped, and it appears on the equation number instead, whenever they are nondimensional. The nondimensional forms of (3.26)-(3.28) are now given as

$$\frac{\partial E_s}{\partial t'} = \frac{\partial}{\partial z}\left(K_s' \frac{\partial E_s}{\partial z}\right) + GK_s' \frac{\partial B}{\partial z} - 6\varepsilon_s', \quad (3.35)^*$$

$$\frac{\partial E_b}{\partial t'} = \frac{\partial}{\partial z}\left(K_b' \frac{\partial E_b}{\partial z}\right) + GK_b' \frac{\partial B}{\partial z} - 6\varepsilon_b', \quad (3.36)^*$$

$$\frac{\partial B}{\partial t'} = \frac{\partial}{\partial z}\left[(K_s' + K_b')\frac{\partial B}{\partial z}\right], \quad (3.37)^*$$

with

$$G = Q / (U^3/L), \quad (3.38)$$

and

$$K_s' = E_s^{1/2} l_{sv}', \quad (3.39)^*$$

$$\varepsilon_s' = E_s^{3/2} l_{sv}'^{-1}, \quad (3.40)^*$$

$$K_b' = E_b^{1/2} l_{bv}', \quad (3.41)^*$$

$$\varepsilon_b' = E_b^{3/2} l_{bv}'^{-1}. \quad (3.42)^*$$

Further, the modification of the vertical length scale under stratification given by (3.18) and (3.25) can be rewritten as

$$l'_{sv} = l'_{sv} / (1 - C_R R_{ib})^{1/2}, \quad (3.43)^*$$

with

$$Ri_b = 3l_{bn}'^2 N^2 / 2E_b, \quad (3.44)^*$$

$$= -\frac{3l_{bn}'^2}{2E_b} G \frac{\partial B}{\partial z} \quad (3.45)^*$$

and

$$l_{sv}' = l_{sn}' / (1 + c_R Ri_s)^{1/2}, \quad (3.46)^*$$

with

$$Ri_s = 3l_{sn}'^2 N^2 / 2E_s, \quad (3.47)^*$$

$$= -\frac{3l_{sn}'^2}{2E_s} G \frac{\partial B}{\partial z}, \quad (3.48)^*$$

where

$$c_R = (a_1/c_1)^2. \quad (3.49)^*$$

The initial conditions are taken as

$$E_s(z,0) = (1+z)^{-2}, \quad (3.50)^*$$

$$E_b(z,0) = (1+H-z)^{-2}, \quad (3.51)^*$$

$$B(z,0) = 0, \quad (3.52)^*$$

which represent the superposition of the turbulent fields generated by the grid-oscillation at the surface and the bottom with no buoyancy flux. It is assumed that the stabilizing buoyancy flux is applied on the surface suddenly at $t' = 0$. The boundary conditions are then given by

$$E_s(H,t') = \alpha, \quad (3.53)^*$$

$$\frac{\partial E_s(0,t')}{\partial z} = 0, \quad (3.54)^*$$

$$\frac{\partial E_b(H,t')}{\partial z} = 0, \quad (3.55)^*$$

$$E_b(0,t') = 1, \quad (3.56)^*$$

$$\frac{\partial B(H,t')}{\partial z} = -[1 + K_b'(H,t)]^{-1}, \quad (3.57)^*$$

$$\frac{\partial B(0,t')}{\partial z} = 0, \quad (3.58)^*$$

where $\alpha (\equiv U_s^2 u_b^2)$ is the ratio of the turbulent kinetic energy at the surface $[U_s^2 \equiv E_s(z=H)]$ to that at the bottom $(U_b^2 \equiv E_s(z=0))$. Here the parameter c_R which represents the effect of stratification on the vertical length scale has been found to be cr=0.1 by Noh and Fernando (1991a) from the comparison of the depth of a thermocline calculated from the model with the experimental data (Kantha and Long 1980, Hopfinger and Linden 1982, Noh and Long 1990). The calculations were performed using an implicit finite-difference method. The height of the water column was fixed as H=100 during the calculation.

4. Dimensional Analysis

When the turbulence generation by grid oscillation exists only at the surface while the stabilizing buoyancy flux is imposed on it, the formation of a therochline is found to be determined by the eddy diffusivity at the surface K_s and the buoyancy flux at the surface Q (Kantha and Long 1980, Hopfinger and Linden 1982, Noh and Long 1990, Noh and Fernando 1991a). This leads to the prediction of the depth of a thermocline Do as

$$D_0 \propto (K_s^3/Q)^{1/4}. \qquad (4.1)$$

In accordance with this it is possible to expect that the phenomena in the presence of the turbulence generation at the bottom will be determined by the eddy diffusivity at the bottom K_b and the height of water column H as well as K_s and Q. That is, the criterion for the formation of a thermocline is determined by

$$f(H, K_b, K_s, Q) = 0. \qquad (4.2)$$

Since they are different only in the proportional constant (i.e., $K_s = c'_\mu K_b'$), the eddy diffusivties K_b and K_s can be replaced by K_b' and K_s', which are variables used in the calculation. That is,

$$f(H, K_b', K_s', Q) = 0. \qquad (4.3)$$

The parameters in (4.3) is then nondimensionalized by K_b' and H to give

$$f\left(\frac{Q}{K_b'^3/H^4}, \frac{K_s'}{K_b'}\right) = 0. \qquad (4.4)$$

Since the length scale of turbulence generated by the grid-oscillation is constant regardless of its frequency and position (Hopfinger and Toly 1976, Hannoun et al 1988), the relation (4.3) can be rewritten as

$$f\left[\left(\frac{H}{L}\right)^3 \frac{HQ}{U_b^3}, \frac{U_s}{U_b}\right] = 0 \qquad (4.5)$$

or

where $\beta \equiv H^4Q/Kb^3 (= (H/L)^3 HQ/Ub^3 = (H/L)^4 G)$. Note that if the effects of the surface mixing is neglected (i.e., $\alpha = 0$), (4.5) redues to the criterion for the stratification (2.2) given by Hopfing and Linden (1982). On the other hand, the same criterion can be expressed by the nondimensionalization in terms of K's and H as

$$f(\alpha, \gamma) = 0, \qquad (4.7)$$

where $\gamma \equiv H^4Q/K_s'^3 = (H/L)^4 G\alpha^{-3/2}$.

The depht of a thermocline D, at which the density jump occurs, can be expressed as

$$D = f(H, K_s', K_b', Q), \qquad (4.8)$$

and can be nondimensionalized in terms of Ks' and Q to give

$$\frac{D}{(K_s'^3/Q)^{1/4}} = f\left[\frac{K_b'}{K_s'}, \frac{H}{(K_s'^3/Q)^{1/4}}\right]. \qquad (4.9)$$

Note that when there is no bottom mixing ($\alpha^{-1} = 0$), the dependence on H in (4.9) disappears.

5.1 Evolutions of buoyancy and turbulent kinetic energy distribution

The results of the time evolutions of the vertical buoyancy distribution $B(z, t')$ are shown in Figute 2 for different values of α for a given $\beta (= 4 \times 10^4)$. When the surface mixing is weak ($\alpha = 0.5$, Figure 2(a)), a thermoc line is developed with time. Most of the buoyancy transfer is limited to the upper layer. Very weak heat transfer across the thermocline exists, however, unlike the case with no bottom mixing (Noh and Fernando 1991a). On the other hand, when the surface mixing is strong ($\alpha = 4.0$, Figure 2(b)), the development of a thermocline is not observed with time. Instead the buoyancy decreases with time uniformly over the whole depth, after the weak exponential buoyancy distribution owing to the turbulent diffusion appears. The rate of the buoyancy decrease at the surface ($z = H$) is much slower in this case than in the case of thermocline formation, as expected from the fact that buoyancy flux is transferred over the whole depth to the bottom.

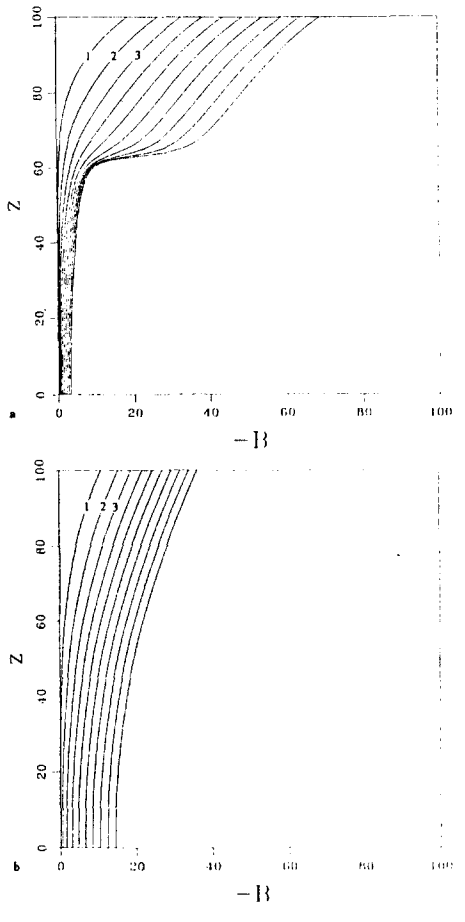

Figure 2. (Continued)

Fig. 2. The evolttions of the vertical distribution of buoyancy with time when $\beta=4\times10^4$. Each graph corresponds $t'=n\triangle t'$ (n=1.. 10, $\triangle t'=200$) : (a) $\alpha=0.5$, (b) $\alpha=4.0$ Hcre z is the vertical distance from the bottom gridoscillkation.

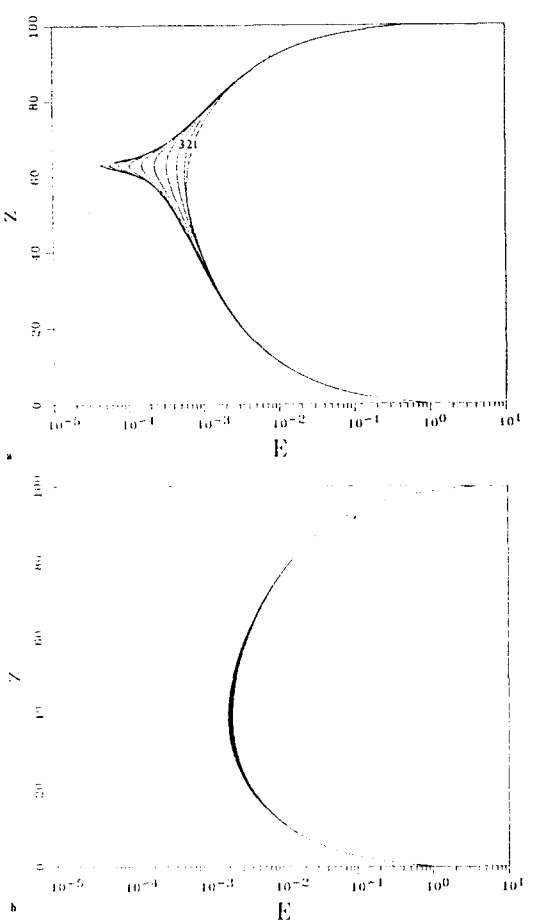

Fig. 3. The evolttions of the turbulent kinetic with time when $\beta=4\times10^4$. Each graph corresponds to $t'=n\triangle t'$ (n=1.. 10, $\triangle t'=200$) : (a) $\alpha=0.5$, (b) $\alpha=4.0$.

Fig. 3 shows the corresponding evolution of turbulent kinetic encrgy $E(=E_b+E_s)$ with time. When a thermicline is not developed, it remains relatively unchanged from the initial state. Meanwhile, when it is developed, it decreases sharply with time at the depth of a thermochine, this suppressing the eddy diffusivity there.

5.2 A criterion for the formation of a thermocline

It is expected that buoyancy difference between the surface and the bottom increases linearly with time for the case of thermocline formation, because buoyancy flux is prohibited at the thermocline; Whereas it remains constant after some time for the well mixed state. Figute 4(a) shows the variations of the buoyancy difference butween the surface and the bottom $\triangle B(\equiv B(O,t')-B(H,t')$ with time for different values of α when $\beta=4\times10^4$. It is found that the value of $\triangle B$ increases linearly with time when a thermocline if formed ($\alpha\leqq1.0$), while it converges to a certain value when the thermocline is not formed ($\alpha\geqq2.0$). The difference between two cases is revealed more clearly in Figure 4(b), where $d\triangle B/dt$ remains at a certain value after some time

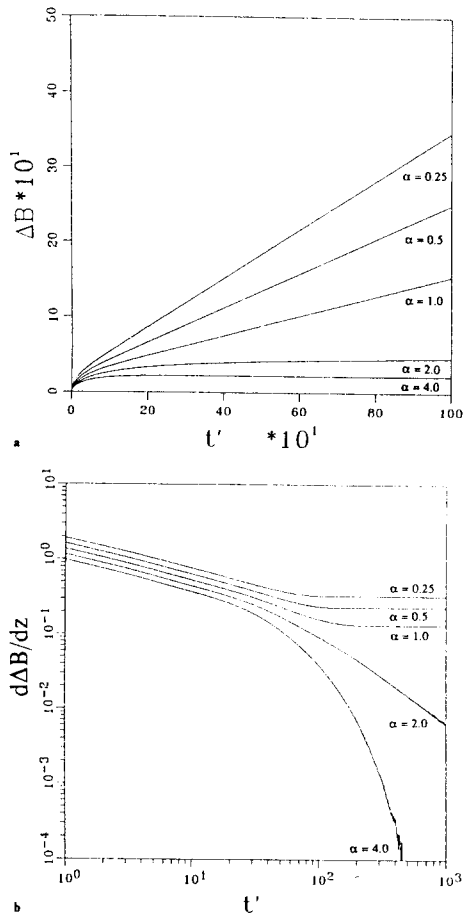

Fig. 4. (a) The variations of the buoyancy difference between the surface and the bottom $\triangle B$ ($\equiv B(O, t') - B(H, t')$ with time for various values of α ($=0.25, 0.5, 1, 2, 4$) when $\beta = 4\times10^4$.
(b) The variations of $d\triangle B/dt$ with time for various values of α ($=0.25, 0.5, 1, 2, 4$) when $\beta = 4\times10^4$.

when $\alpha \leqq 1.0$, Whereas it decreases continuously with time when $\alpha \geqq 2.0$. From this it is possible to discern the case of thermocline formation (' the stratified state ') from that of no formation (' the well-mixed state ').

Careful inspection of Figure 2 also reveals interesting features which help to find the criterion for the formation of a thermocline. When there is no thermocline, the maximum of the buoyancy gradient dB/dz always remains at the surface. On the other hand, when a thermocline appears, it jumps to the position of a thermocline. The variation of the depth of the maximum density gradient D_t with time is shown if Figure 5 for the corresponding cases of Figure 4.

Figure 6 shows a criterion predicting the formation of a thermocline, obtained from the procedures described above. For a given β, the maxmum/minimum value of α computed

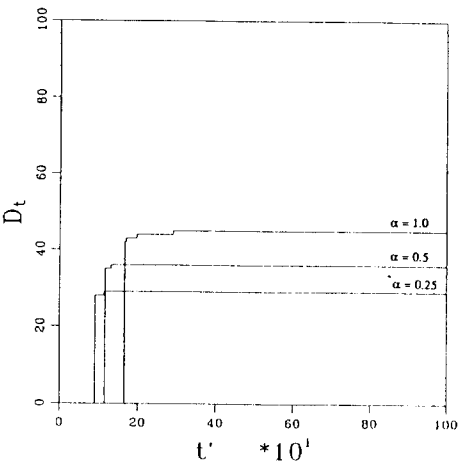

Fig. 5. The variations of the position of the maximum buoyancy gradient with time for various values of α ($=0.25, 0.5, 1, 2, 4$) when $\beta = 4\times10^4$.

without/with the formation of a thermocline is indicated by a horizontal bar. It is found that the critical values of β for the transition increases with α. This means that the well-mixed layer is more likely to occr as α becomes larger. Depth of the potential thermocline formation is decreased with the decrease of α for a given value of β. As the distance from the turbulence source at the bottom to the position of thermocline formation increases, smaller turbulence kinetic energy is supplied there so that it becomes more difficult to disrupt the formation of a thermocline. Dependence on α is found to become weaker, however, when β is small ($\beta < 10^2$). This suggests that, if β becomes sufficiently small, the bottom mixing itself becomes strong enough to mix the whole water column regardless of the surface mixing.

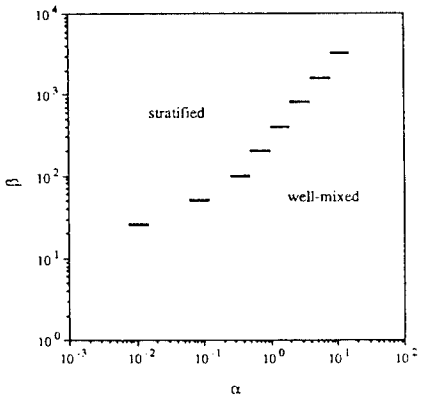

Fig. 6. Criterion for the formation of a front in terms of α and β. For a given β, the maximum/minimum value of α computed without/with the formation of a thermocline is indicated by a horizontal bar.

The effects of bottom mixing can be clearly illustrated, if the equations are calculated in terms of α and γ. The results are shown in Figure 7. It shows that the thermocline, which is always formed at a depth Do in the absence of bottom mixing ($\alpha^{-1}=O$) as long as Do<H (Noh and fernando 1991a), is disrupted, if the bottom mixing becomes stronger than the critical values.

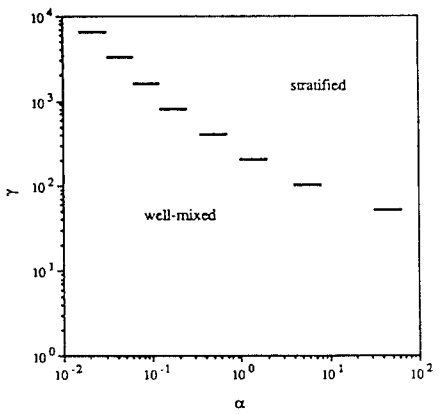

Fig. 7. Criterion for the formation of a front in terms of α and γ. For a given γ, the maximum/minimum value of α computed without/with the formation of a thermocline is indicated by a horizontal bar.

5. 3. The depth of a thermocline

The depth of thermocline D_t can be defined as the depth of the maximum density gradient, and its equilibrium depth D is obtained from the limiting value of D as t ' goes to infinity. In practice, as is shown in Figure 5, the calculations clearly shows the convergence of D_t to an asymptotic value corresponding to D soon after the first appearance of non-zero D $_t$. The calculations were made until $dD_t/dt < 10^{-3}$.

Figure 8 shows that the variation of D with α for given values of γ ($\gamma=4\times10^4$, 16×10^4). Here the case $\alpha^{-1}=O$ represents the formation of a thermocline without turbulence source at the bottom, whose value of D can be predicted by (4. 1). It is interesting to observe that D decreases with the increase of the bottom mixing. As the weak density stratification is developed to form a thermocline, it is exposed to the erosion from below by the bottom mixing. This may cause the upward shift of the position of a thermocline. It is also found that D is more sensitive to α, when D is large so that the position of a thermocline is closer to the bottom.

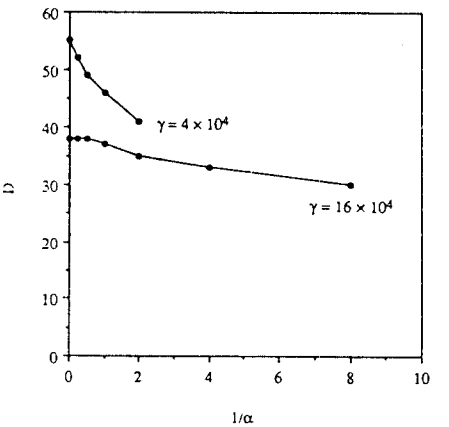

Fig. 8. The variations of the depth of the thermocline D with α.

6. Interpretation

The importance of the surface mixing for the prediction of stratification was first considered by Fearnhead (1975), who correctly suggested that the required work to maintain the well-mixed stated is for the potential energy difference ϕ between the wellmixed state and the stratified state with a thermocline at z=H-Do such as

$$\phi = \tfrac{1}{2} BD_0(H - D_0). \tag{6.1}$$

The rate of working required to maintain the mixed state is then given by

$$\frac{d\phi}{dt} = \tfrac{1}{2} Q(H - D_0), \tag{6.2}$$

from Q=d(BDo)/dt and dDo/dt=0.

The turbulent kinetic energy flux from the bottom F_b calculated from

$$F_b = \frac{\partial}{\partial z}\left(K_b \frac{\partial E_b}{\partial z}\right), \tag{6.3}$$

gives

$$F_b(z=O) \sim U_b^3. \tag{6.4}$$

It has been suggested by Fearnhead (1975) that the criterion for the formation of a thermocline is determined by the parameter $R\delta o$ using the kinetic energy flux near the bottom $F_b(z=O)$. In this case R can be expressed as

$$R_{\delta o} \sim \frac{d\phi/dt}{F_b(z=0)} \tag{6.5}$$

$$\sim Q(H - D_0)/U_b^3 \tag{6.6}$$

$$\sim \beta' \delta, \tag{6.7}$$

where $\delta = 1 - Do/H$ and $\beta' = QH/U_b^3 = (H/L)^{13} \beta$. Since H was fixed during the calculation, β' is proportional to β, so $R\delta o \propto \beta\delta$. Figure 9 shows the replot of Figure 6 (or Figure 7) in terms of β and δ. It does not follow the prediction given by (6.7), but the critical values of β decreases much faster with δ.

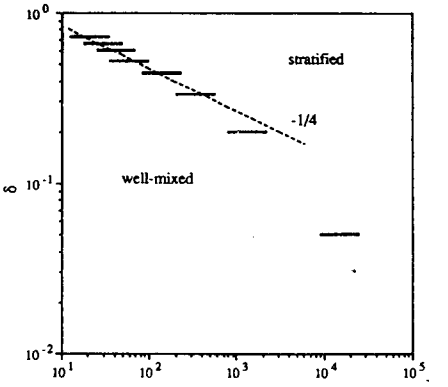

Fig. 9. Criterion for the formation of a front in terms of β and δ. The dashed line represents the relation given by (5.10).

Hopfinger and Linden (1982) proposed that the local r.m.s. turbulent velocity is more relevant to the formation of stratification as suggested by (2.3). In the same way it appears more reasonable to presume that what is important to obstruct the thermocline formation is the turbulent kinetic energy flux near the position of the thermocline formation rather than that near the bottom. The parameter is then modified as

$$R_\delta \sim \frac{d\phi/dt}{F_b(z = H - D_0)} \tag{6.8}$$

$$\sim \frac{Q(H - D_0)}{|K_b/(H - D_0)|^3} \tag{6.9}$$

$$\sim \beta\delta^4, \tag{6.10}$$

using the characteristic of the r.m.s. turbulent velocity.

A good agreement is observed between (6.10) and Figure 9, when δ is larger than 0.5. As β approaches) however, the dependence on δ decreases from the same reason as discussed in section 5.2.

7. Conclusion and Discussion

In the previous sections, a numerical model was presented to describe the formation of a thermocline in a water columm, where shear-

free turbulence is generated from both the surface and the bottom and a stabilizing buoyancy flux is imposed on the surface for the purpose of understanding the formation of a tidal front. The one-dimensional turbulence model, which was based on the turbulence generated by the grid-oscillation, took account of the interaction between the turbulence structure and the stratification of fluid.

The time evolutions of the verical distribution of density and turbulent kinetic energy calculated from the model shows that the emergence of a thermocline depends on the conditions determined by the buoyancy flux at the surface Q, the eddy diffusivities maintained at the bottom and at the surface K_b and K_s, respectively, and the depth of the water column H. The criterion for the formation of a thermocline was predicted as R $\delta^4\sim$ constant for large δ ($\delta>0.5$), but the dependence on δ decreases as δ approach O, where $R=H^4Q/K_b^3$, $\delta=1-Do/H$ and Do is the depth of a thermocline in the absence of bottom mixing. The result shows that the onset of stratification is determined by the balance between the rate of potential energy increases required to maintain the well-mixed state and the turbulent kinetic energy flux near the position of a thermocline formulation, rather than that near the bottom, as suggested in the previous studies. The depth of a thermocline was found to decrease as the bottom mixing increases for a given value of D_o. This may be caused by the erosion from below due to the bottom mixing, as the weak density stratification is developed to form a thermocline.

In the oceanic mixed layer turbulence is generated by the vertical shear of the mean flow within the mixed layer as well as by the propagation of the turbulent kinetic energy from the sea surface. According to Niiler and Kraus (1977), however, the former is generally negligible compared with the latter in the oceanic mixed layer. Although the role of the vertical shear of the mean flow may be important in the bottom boundary layer close to the bottom (Heathershaw 1979), the turbulence from the bottom is important only to determine the level of turbulence at the thermocline as shown in section 6. It is thus expected that the same mechanism as shown in this paper determines the stratification/destratification of the mixed layer. Inclusion of such effects as the vertical shear of the mean flow and modification of the velocity and length scales of turbulence ((3.16), (3.17), (3.21) and (3.22)) in accordance with the oceanic data are necessary, however, to apply the model to the tidal front in the ocean. In the future study these factors can be taken into consideration, whose results will be compared directly with the observation data such as (2.1).

References

Andre, J.C., De Moor, G., Lacarrere, P., Therry, G. and du Vachat, R. "Modeling the 24hour evolution of the mean and turbulent structures of the planetary boundary layer," J. Atmos. Sci. 35, 1861~1883 (1978).

Batchelor, G.K., An Introduction to Fluid Dynamics, Cambridge University Press (1967).

Britter, R.E., Hunt, J.C.R., Marsh, G.L. and Snyder, W.H., "The effects of stable stratification on turbulent diffusion and the decay of grid turbulence," J. Fluid Mech. 127, 27~44 (1983).

Bye, J.A.T., "Richardson number profiles in laboratory experiments applied to shallow seas," Geophys. Astrophys. Fluid Dyn. 51, 135~166 (1990).

Csanady, G.T., "Turbulent diffusion in a stratified fluid," J. Atmos. Sci. 21, 439~447 (1964).

Fearnhead, P.G., "On the formation of fronts by tidal mixing around the British Isles," Deep Sea Res. 22, 331~321 (1975).

Fedorov, K.N., The Physical Nature and Structure of Ocean Fronts, Springer Verlag (1983).

Galperin, G., Rosati, A., Kantha, L.H. and Mellor, G.L., "Modeling rotating stratified turbulent flows with application to oceanic mixed layers," J. Phys. Ocean. 19, 901~916 (1989).

Hannoun, I.A., Fernando, H.J.S. and List, E.J., "Turbulence near a sharp density interface," J. Fluid Mech. 189, 189~209 (1988).

Heathershaw, A.D., "The turbulent structure of the bottom boundary layer in a tidal current," Geophys. J.R. Astro. Soc. 58, 395~430 (1979).

Hopfinger, E.J. and Linden P.F., "Formation of thermoclines in zero-mean-shear turbulence," J. Fluid Mech. 114, 157~173 (1982).

Hopfinger, E.J. and Toly, J.A., "Spatially decaying turbulence and its relation to mixing across density interface," J. Fluid Mech, 78, 155~175 (1976).

Kantha, L.H. and Long, R.R., "Turbulent mixing with stabilizing surface buoyancy flux," Phys. Fluids 23, 2142~2143 (1980).

Niiler, P.P. and Kraus, E.B., "One-dimensional models of the upper ocean," Modelling and Prediction of the Upper Layer of the Ocean (ed. E.B. Kraus, Pergamon Press), pp. 143~172 (1977).

Noh, Y. and Fernando, H.J.S., "A numerical study on the formation of a thermocline in shear-free turbulence," Phys. Fluids A3, 422~426 (1991a).

Noh, Y. and Fernando, H.J.S., "Dispersion of suspended particles in turbulent flow," Phys. Fluids A3, 1730~1740 (1991b).

Noh, Y. and Long, R.R., "Turbulent mixing in a rotating, stratified fluid," Geophys. Astrophys. Fluid Dyn. 53, 125~143 (1990).

Pearson, H.J., Puttock, J.S. and Hunt, J.C.R., "A statistical model of fluid-element motions and vertical diffusion in a homogeneous stratified turbulent flow," J. Fluid Mech. 129, 219~249 (1983).

Pingree, R.D. and Griffith, D.K., "Tidal fronts on the shelf seas around the British Isles," J. Geophys. Res. 83, 4615~4622 (1978).

Simpson, J.H. and Hunter, J.H., "Fronts in the Irish Sea," Nature 250, 404~406 (1974).

Simpson, J.H., Allen, C.M. and Morris, N.C.G., "Fronts on the continental shelf," J. Geophys. Res. 83, 4607~4614 (1978).

Turner, J.S., "Turbulent entrainment: the development of the entrainment assumption, and its application to geophysical flows," J. Fluid Mech. 173, 431~471 (1986).